

Solution of the time-dependent diffusion equation for layered diffusive media by the eigenfunction method

Fabrizio Martelli,^{1,*} Angelo Sassaroli,^{2,†} Samuele Del Bianco,¹ Yukio Yamada,³ and Giovanni Zaccanti¹

¹*Dipartimento di Fisica dell'Università degli Studi di Firenze and Istituto Nazionale per la Fisica della Materia, Via G. Sansone 1, 50019 Sesto Fiorentino, Firenze, Italy*

²*Institute for Human Science and Biomedical Engineering, National Institute of Advanced Industrial Science and Technology, Namiki 1-2, Tsukuba, Ibaraki 305-8564, Japan*

³*Department of Mechanical Engineering and Intelligent Systems, University of Electro-Communications, Chofugaoka, 1-5-1 Chofu, Tokyo 182-8585, Japan*

(Received 20 May 2002; published 27 May 2003)

An exact solution of the time-dependent diffusion equation for the case of a two- and a three-layered finite diffusive medium is proposed. The method is based on the decomposition of the fluence rate in a series of eigenfunctions and upon the solution of the consequent transcendental equation for the eigenvalues obtained from the boundary conditions. Comparisons among the solution of the diffusion equation and the results of Monte Carlo simulations show the correctness of the proposed model.

DOI: 10.1103/PhysRevE.67.056623

PACS number(s): 05.60.-k, 42.25.Dd

I. INTRODUCTION

The problem of light propagation through random media bounded by parallel planes has been a subject of interest for decades because many physical systems are likely to be represented in this way [1,2]. The radiative transfer equation (RTE) [1–3] that is derived in transport theory has been widely studied because usually it is simpler than the equations derived in the analytical theory [2], and its predictions have been tested in many situations of interest. However, the RTE is a complex integro-differential equation that is usually solved by resorting to some numerical methods or to some approximations. Applications of the RTE to the study of light propagation in a sequence of turbid slabs can also be found in the literature [1,2,4,5] because many physical systems (e.g., atmosphere, biological tissues) are better described if we consider a layered structure. However, to date, almost all the studies involving the RTE were concerned with a plane wave source and a steady state propagation. Moreover, the approximate solutions of the RTE proposed in the literature require much computational effort and are not straightforward to be used. If we consider the diffusion approximation [2,3] to the RTE, analytical solutions for homogeneous media have been obtained also for the time domain (TD) [6] and the frequency domain (FD) [7] diffusion equation (DE) and for pointlike sources. The time domain and the frequency domain Green's functions of DE in different geometries can be found in Ref. [8].

When the nature of randomness is such that diffusion conditions hold, it is possible to use the DE to describe light propagation [2]. In the recent years, there has been an enhanced interest to study the problem of light propagation in

layered random media, also for its applications in the field of tissue optics. In fact, many biological tissues are likely to be described by a sequence of diffusive layers having different optical parameters and more accurate clinical information can be gained from such a modeling of tissues. Some authors [9–11] investigated the limitations of mathematical models that do not take into account the layered structure of tissues. Several studies for layered media have been carried out either in the continuous wave (CW) domain [12–20] or in the FD [15,21–25] by using different methods: analytical solution of DE, random walk, Monte Carlo (MC) method, and finite element method. In these papers, the authors provided different formulas only for infinitely extended slabs, and in most cases for a medium composed of a finite slab on top of a semi-infinite medium. Although interesting results were found, the proposed methods suffer from several drawbacks: numerical methods are usually time consuming, and the analytical solutions of DE proposed in most of the CW and FD studies are not expressed in a closed form, and numerical integration of an inverse space-transverse Fourier transform is usually required. It might be impractical to implement inversion procedures for the *in situ* or *in vivo* determination of the optical properties based on these models.

By using different methods also in TD, some studies have been carried out [14,26–30]. The particular interest for time domain investigations is focused mainly to find correct and efficient methods to calculate the Green's function of a system and to implement fast and reliable inversion procedures. However, despite the important role that analytical solutions of the time domain DE have, only a few studies presented useful expressions for layered media. Dayan *et al.* [14] found approximate expressions of the Green's function for the case of a slab on top of a semi-infinite medium. In the work of Kienle *et al.* [27], explicit time domain formula for the Green's functions were not given and numerical calculations of inverse space-transverse and inverse time Fourier transform were required. Tualle *et al.* [28] used an extension of the method of images to calculate the real space Green's function for a layered medium. However, the expressions, even for a simplified medium composed by one layer on top of a semi-infinite medium, were obtained after several diffi-

*Email address: fabrizio.martelli@unifi.it

†Present address: Department of Biomedical Engineering, Bioengineering Center, Tufts University, 4 Colby Street, Medford, Massachusetts 02155.

cult mathematical steps. Martelli *et al.* [30] used approximate boundary conditions to solve the time-dependent DE with the eigenfunction method. Early studies that used a similar method are the works of Takatani and Graham [12] and Schmitt *et al.* [13], however both of them were concerned with the steady state DE.

The many papers on the topic of light propagation in layered random media testify that there is no general agreement about the choice of the mathematical procedures to obtain relatively simple equations that can be easily integrated and that can lead to useful and straightforward expressions of immediate interpretation. In this work, we present a fast method to solve the time-dependent DE for a layered finite medium. We provide an exact expression of the Green's function, which is easily calculated by using the eigenfunction method. The proposed method is an extension of that one used in a previous paper [30], but here exact boundary conditions are considered. The key point of the method is the solution of a transcendental equation for the eigenvalues that can be accomplished with classical methods in a short time (within few seconds by using a Pentium IV 1.8 GHz). We stress the importance of imaginary roots of the transcendental equation that to the best of our knowledge, were not mentioned by previous authors. We have found that without including the imaginary roots of the transcendental equation, the calculation of the Green's function cannot be carried out correctly. The information obtained in this preliminary step is used to calculate in a short time a wide set of Green's functions at different source-detector distances. We can say that all the information relevant for the problem is contained only in the set of eigenvalues. The expression of the Green's function and its mathematical dependence on the optical properties of the medium is quite straightforward and easy to be interpreted; time integration and Fourier transform of the Green's function can be easily carried out to yield exact expressions in CW and FD. An evidence of the correctness of our model is provided by comparison with MC results.

We also notice that the other models quoted above were proposed for more restricted geometries. For example, one common element is the requirement that the layered medium is laterally infinitely extended. Here, we provide the solution for a layered parallelepiped; however, we remark that other finite layered geometries (e.g., cylindrical) can be solved with the same method. The formulas have been obtained by using the extrapolated boundary condition (EBC) [31] at the upper and lower surfaces of the parallelepiped and the zero boundary condition (ZBC) [6] at the lateral surfaces of the parallelepiped. Rigorous boundary conditions have been used between the diffusive layers. Moreover, although the expressions are found for a pointlike source, expressions for an isotropic line source can also be easily derived. In Appendix D, the exact theory of a three-layered medium is also described.

We have implemented a fitting procedure based on the formulas presented for the retrieval of the optical properties of the medium starting from a single measurement of reflectance. Fitting procedures on measurements simulated by MC results have been carried out. The convergence of the procedure and the retrieval of the optical properties could be ob-

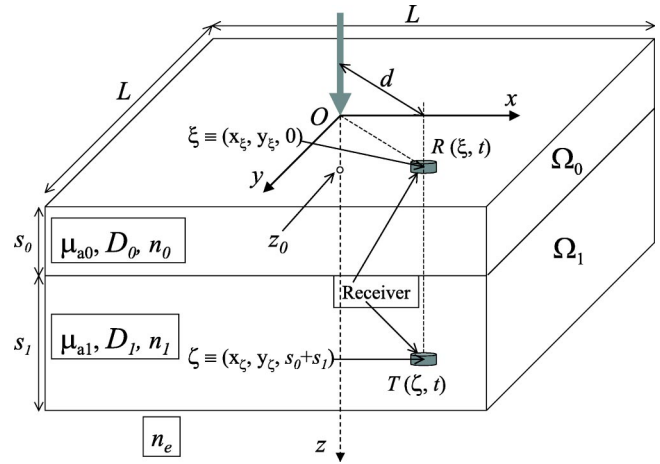


FIG. 1. A two-layered parallelepiped with a laser beam impinging on the upper surface. L is the lateral size along both x and y axes; s_0 and s_1 are the thicknesses of the top and bottom layers, respectively; μ_{a0} and μ_{a1} are the absorption coefficients; and D_0 and D_1 are the diffusion factors of the first and the second layer, respectively. $R(\xi, t)$ and $T(\zeta, t)$ are the reflectance and transmittance calculated at two arbitrary points ξ and ζ on the upper and lower surfaces, respectively.

tained in few minutes. This result testifies the potentiality of the formulas for the inverse problem devoted to the reconstruction of the optical properties of an unknown medium.

In Sec. II and in Appendixes A–E the theory of the work is described. In Sec. III, comparisons between the analytical theory and MC results are presented. Conclusions are given in Sec. IV.

II. THEORY

The eigenfunction method offers a very useful way to solve partial differential equations, either of hyperbolic, parabolic, or elliptic type [32–34]. In this work, we are concerned with the parabolic-type time-dependent DE, which is usually derived from the RTE [3]. The DE and, in general, parabolic equations can also be derived from very general principles of energy and photon flux balance within a region having smooth optical properties, though in general not homogeneous, if we assume that the flux vector $\mathbf{J}(\mathbf{r}, t)$ and the irradiance $\Phi(\mathbf{r}, t)$ are related by Fick's law: $\mathbf{J}(\mathbf{r}, t) = -D(\mathbf{r})\nabla\Phi(\mathbf{r}, t)$ (Ref. [32], pp. 163–165). If the smoothness requirement is not met throughout the whole region, as for the case of a sharp change in the optical properties across a plane, the general balance principles can be used to derive matching conditions for the solutions of the parabolic equations that are valid on both sides of the plane (Ref. [32], p. 325). In particular, we are interested in studying the time-dependent DE for a two-layered parallelepiped for the case of an isotropic Dirac- δ source term.

Figure 1 shows the medium Ω composed of two regions: $\Omega = \Omega_0 \cup \Omega_1$. In the figure, s_0 and s_1 are the thicknesses, μ_{a0} and μ_{a1} are the absorption coefficients, D_0 and D_1 are the diffusion coefficients, and n_0 and n_1 are the absolute refractive indices of the first and second layers, respectively. n_e is the absolute refractive index of the surrounding me-

dium. The size of the medium along x and y axes is assumed to be L . The origin of the reference system is chosen as the point where a collimated laser beam (z axis) impinges the medium, therefore its physical boundaries belong to the planes $x = \pm L/2$, $y = \pm L/2$, and $z = 0$, $z = s_0 + s_1$. Let us consider at first that the source term is represented by a single isotropic point source placed in $\mathbf{r}_0 = (0, 0, z_0)$, i.e., $S(\mathbf{r}, t) = \delta(\mathbf{r} - \mathbf{r}_0) \delta(t)$. Later, the case of a collimated laser beam will be discussed. For the moment, we restrict our investigation to a single point source located in the first layer. The case of a single point source located in the second layer will be considered later on. The diffusion equation for the irradiance is written as (v is the speed of the light)

$$\left[\frac{1}{v} \frac{\partial}{\partial t} + \mu_a - \nabla [D(\mathbf{r}) \nabla] \right] \Phi(\mathbf{r}, t) = \delta(\mathbf{r} - \mathbf{r}_0) \delta(t). \quad (1)$$

Because of the discontinuities of the optical properties across the plane $z = s_0$, we expect to find a solution of Eq. (1) having some discontinuities. The proposed method to solve the problem is an extension of the one proposed by Zauderer (Ref. [32], pp. 335–338). The problem must be separated in the two layers and can be stated as an initial-boundary value problem as the following:

$$\begin{aligned} [\partial/(v \partial t) + \mu_{a0} - D_0 \nabla^2] \Phi_0(\mathbf{r}, t) &= 0, \\ t > 0, \quad 0 \leq z \leq s_0, \end{aligned} \quad (2)$$

$$\begin{aligned} [\partial/(v \partial t) + \mu_{a1} - D_1 \nabla^2] \Phi_1(\mathbf{r}, t) &= 0, \\ t > 0, \quad s_0 \leq z \leq s_0 + s_1, \end{aligned}$$

and the initial-boundary value conditions:

$$\begin{aligned} \Phi_0 \left(x = \pm \frac{L}{2}, y, z, t \right) &= \Phi_0 \left(x, y = \pm \frac{L}{2}, z, t \right) \\ &= \Phi_0(x, y, z = -2A(n)D_0, t) = 0, \end{aligned} \quad (3)$$

$$\begin{aligned} \Phi_1 \left(x = \pm \frac{L}{2}, y, z, t \right) &= \Phi_1 \left(x, y = \pm \frac{L}{2}, z, t \right) \\ &= \Phi_1(x, y, z = s_0 + s_1 + 2A(n)D_1, t) \\ &= 0, \end{aligned} \quad (4)$$

$$\Phi(\mathbf{r}, t = 0) = v \delta(\mathbf{r} - \mathbf{r}_0). \quad (5)$$

Equation (5) represents the initial distribution of sources in the medium. Equations (3) and (4) represent the boundary conditions with the external medium and are based on two different assumptions: the EBC [31] has been used on the upper and lower surfaces ($z = 0$ and $z = s_0 + s_1$), while the ZBC [6,31] has been used at the lateral boundaries $x = \pm L/2$ and $y = \pm L/2$. With the EBC, the fluence rate is assumed equal to zero at an extrapolated boundary outside the turbid medium at a distance $z_e = 2AD$. The coefficient $A(n)$ also includes the effect of reflections due to the refractive index mismatch n between the medium and the surroundings [31]. The ZBC simply assumes the fluence rate

equal to zero at the physical boundary of the medium. The ZBC is more approximated [31], however, its use on the lateral boundary significantly simplifies the problem here addressed, since it leads the fluence rate to vanish on the lateral physical boundaries of the diffusive layers. On the other hand, with the EBC we would obtain different lateral extrapolated boundaries in the different layers. The boundary conditions at the lateral boundary does not affect the reflectance and the transmittance, unless the source or the receiver is close to the boundary. In the stated problem, we have assumed that the refractive index of the diffusive medium is constant, however the theory can be easily extended for a more general case [35].

The matching conditions for this problem are derived from the continuity of the irradiance and of the photon flux at the boundary $z = s_0$:

$$\begin{aligned} \Phi_0(x, y, z = s_0, t) &= \Phi_1(x, y, z = s_0, t), \\ D_0 \partial \Phi_0(x, y, z = s_0, t) / \partial z &= D_1 \partial \Phi_1(x, y, z = s_0, t) / \partial z. \end{aligned} \quad (6)$$

We will search for a solution of the stated problem of the kind

$$\Phi(\mathbf{r}, t) = \begin{cases} \Phi_0(\mathbf{r}, t) = \rho_0(\mathbf{r}) \eta(t), & 0 \leq z \leq s_0 \\ \Phi_1(\mathbf{r}, t) = \rho_1(\mathbf{r}) \eta(t), & s_0 \leq z \leq s_0 + s_1. \end{cases} \quad (7)$$

It is in fact obvious that the temporal evolution of Φ_0 and Φ_1 must be coincident if we want that condition (6) be valid. We will also require that the functions $\rho_0(\mathbf{r})$ and $\rho_1(\mathbf{r})$ satisfy conditions (3) and (4). After substitution of expression (7) in system (2), we are led to the following eigenvalue problem:

$$\begin{aligned} d\eta(t)/dt &= -\lambda \eta(t), \\ -D_0 \nabla^2 \rho_0(\mathbf{r}) + \mu_{a0} \rho_0(\mathbf{r}) &= \lambda/v \rho_0(\mathbf{r}), \\ -D_1 \nabla^2 \rho_1(\mathbf{r}) + \mu_{a1} \rho_1(\mathbf{r}) &= \lambda/v \rho_1(\mathbf{r}). \end{aligned} \quad (8)$$

System (8) can also be rewritten as

$$\begin{aligned} d\eta(t)/dt &= -\lambda \eta(t), \\ \nabla^2 \rho_0(\mathbf{r}) + K_0^2 \rho_0(\mathbf{r}) &= 0, \\ \nabla^2 \rho_1(\mathbf{r}) + K_1^2 \rho_1(\mathbf{r}) &= 0, \end{aligned} \quad (9)$$

where K_0^2 and K_1^2 are given by the expressions

$$K_0^2 = \left(\frac{\lambda}{v} - \mu_{a0} \right) / D_0, \quad K_1^2 = \left(\frac{\lambda}{v} - \mu_{a1} \right) / D_1. \quad (10)$$

We note that because the diffusion operator is self-adjoint and positive (Ref. [32], pp. 171–178), the parameter λ is real and non-negative. On the contrary, no assumption can be made on the sign of K_0^2 and K_1^2 , and in general the Helmholtz equations [34] in system (9) admit solutions both for positive and negative values of these parameters.

In order to solve the Helmholtz equations in system (9), we use the separation of variables method, as shown in Appendix A for the case of a homogeneous cube. The procedure

reported in Appendix A can also guide us to search for possible solutions of the Helmholtz equations in system (9), and therefore to find the proper eigenfunctions of the whole medium. In fact, let us assume that a complete orthonormal set of eigenfunctions is given by the expression

$$\rho_{lmn}(\mathbf{r}) = \frac{1}{N_{lmn}} \times \begin{cases} \rho_{0lmn} = \cos(K_l x) \cos(K_m y) a_{n0} \cos(K_{n0} z + \gamma_{n0}), & 0 \leq z \leq s_0 \\ \rho_{1lmn} = \cos(K_l x) \cos(K_m y) a_{n1} \cos(K_{n1} z + \gamma_{n1}), & s_0 \leq z \leq s_0 + s_1, \end{cases} \quad (11)$$

where N_{lmn} is a normalizing factor and a_{n0}, a_{n1} are coefficients to be determined. From the separation of variables method, it is clear that K_l and K_m are the ones found for the homogeneous cube:

$$K_l = (2l - 1)\pi/L, \quad l = 1, 2, 3, \dots, \quad (12)$$

$$K_m = (2m - 1)\pi/L, \quad m = 1, 2, 3, \dots,$$

and that the conditions

$$\begin{aligned} K_0^2 &= K_l^2 + K_m^2 + K_{n0}^2, \\ K_1^2 &= K_l^2 + K_m^2 + K_{n1}^2 \end{aligned} \quad (13)$$

must be satisfied. We note that Eqs. (11) satisfy the boundary conditions (3) and (4), if γ_{n0} and γ_{n1} are chosen as

$$\begin{aligned} \gamma_{n0} &= 2K_{n0}AD_0 + \pi/2, \\ \gamma_{n1} &= -K_{n1}(s_0 + s_1 + 2AD_1) + \pi/2. \end{aligned} \quad (14)$$

The matching conditions (6) applied to ρ_{0lmn} and ρ_{1lmn} yield the linear system of equations for a_{n0} and a_{n1} :

$$\begin{aligned} a_{n0} \sin[K_{n0}(s_0 + 2AD_0)] + a_{n1} \sin[K_{n1}(s_1 + 2AD_1)] &= 0, \\ a_{n0} D_0 K_{n0} \cos[K_{n0}(s_0 + 2AD_0)] \\ - a_{n1} D_1 K_{n1} \cos[K_{n1}(s_1 + 2AD_1)] &= 0. \end{aligned} \quad (15)$$

System (15) admits nontrivial solutions ($a_{n0}, a_{n1} \neq 0$), if and only if the determinant vanishes. Therefore, we are led to the transcendental equation for the eigenvalues:

$$\begin{aligned} \frac{1}{D_0 K_{n0}} \tan[K_{n0}(s_0 + 2AD_0)] \\ = - \frac{1}{D_1 K_{n1}} \tan[K_{n1}(s_1 + 2AD_1)]. \end{aligned} \quad (16)$$

We will come back to study this equation later on when the different possibilities that arise from the boundary conditions will be clear. Let us now consider the temporal evolution of the irradiance, which is obtained by solving the first equation in system (9). Because there is a discrete set of eigenvalues λ_{lmn} defined by Eq. (10), we can write a general solution of the equation for $\eta(t)$ as

$$\eta_{lmn}(t) = \eta_{lmn}(t=0) \exp(-\lambda_{lmn}t). \quad (17)$$

The general solution of our initial-boundary value problem can be written as [32–34]

$$\Phi(\mathbf{r}, t) = \sum_{l,m,n=1}^{\infty} \eta_{lmn}(t=0) \rho_{lmn}(\mathbf{r}) \exp(-\lambda_{lmn}t). \quad (18)$$

The initial condition (5) is used to determine $\eta_{lmn}(t=0)$. It gives

$$\Phi(\mathbf{r}, t=0) = v \delta(\mathbf{r} - \mathbf{r}_0) = \sum_{l,m,n=1}^{\infty} \eta_{lmn}(t=0) \rho_{lmn}(\mathbf{r}), \quad (19)$$

and by using the orthonormality of the eigenfunctions we have

$$\begin{aligned} \eta_{lmn}(t=0) &= (\Phi(\mathbf{r}, t=0), \rho_{lmn}(\mathbf{r})) \\ &= \int_{\Omega_e} v \delta(\mathbf{r} - \mathbf{r}_0) \rho_{lmn}^*(\mathbf{r}) d\mathbf{r}, \end{aligned} \quad (20)$$

where we have used the definition of the scalar product in the space of the continuous functions in the region of the extrapolated parallelepiped [$\rho_{lmn}^*(\mathbf{r})$ is the complex conjugate of $\rho_{lmn}(\mathbf{r})$]. The reason why we have used the general definition of the scalar product valid for complex functions is that we allow for the possibility that the component along the z axis of the solutions of the Helmholtz equations in system (9) is given by a combination of exponential functions. This possibility had to be discarded for the case of a homogeneous cube as shown in Appendix A. The expression of $\rho_{lmn}(\mathbf{r})$ in Eqs. (11) can include also this possibility only if the components along the z axis are complex functions. We remind that when the argument of a sinusoidal function is complex, we obtain a linear combination of hyperbolic functions. The choice of the coefficients a_{n0} and a_{n1} together with the boundary conditions assure that $\rho_{lmn}(\mathbf{r})$ is a set of real and orthonormal functions [see Appendix B for the proof of the orthonormality of the eigenfunctions $\rho_{lmn}(\mathbf{r})$]. Substituting expression (11) in Eq. (20), we have

$$\eta_{lmn}(t=0) = v \rho_{lmn}^*(\mathbf{r}_0) = v a_{n0}^* \cos^*(K_{n0}z_0 + \gamma_{n0}) / N_{lmn}. \quad (21)$$

Finally, we are able to write the solution of our initial-boundary value problem as

$$\Phi(\mathbf{r}, t) = \begin{cases} \sum_{l,m,n=1}^{\infty} v \cos(K_l x) \cos(K_m y) |a_{n0}|^2 \cos(K_{n0} z + \gamma_{n0}) \\ \times \cos^*(K_{n0} z_0 + \gamma_{n0}) \exp[-(K_0^2 D_0 + \mu_{a0}) v t] / N_{lmn}^2, & 0 \leq z \leq s_0 \\ \sum_{l,m,n=1}^{\infty} v \cos(K_l x) \cos(K_m y) a_{n0}^* a_{n1} \cos(K_{n1} z + \gamma_{n1}) \\ \times \cos^*(K_{n0} z_0 + \gamma_{n0}) \exp[-(K_1^2 D_1 + \mu_{a1}) v t] / N_{lmn}^2, & s_0 \leq z \leq s_0 + s_1. \end{cases} \quad (22)$$

The coefficients a_{n0} and a_{n1} , according to system (15), are not uniquely determined; however, their ratio is determined by the continuity of the irradiance. We can rewrite Eq. (22) as

$$\Phi(\mathbf{r}, t) = \begin{cases} \sum_{l,m,n=1}^{\infty} v \cos(K_l x) \cos(K_m y) \cos(K_{n0} z + \gamma_{n0}) \\ \times \cos^*(K_{n0} z_0 + \gamma_{n0}) \exp[-(K_0^2 D_0 + \mu_{a0}) v t] / \tilde{N}_{lmn}^2, & 0 \leq z \leq s_0 \\ \sum_{l,m,n=1}^{\infty} v \cos(K_l x) \cos(K_m y) b_{n1} \cos(K_{n1} z + \gamma_{n1}) \\ \times \cos^*(K_{n0} z_0 + \gamma_{n0}) \exp[-(K_1^2 D_1 + \mu_{a1}) v t] / \tilde{N}_{lmn}^2, & s_0 \leq z \leq s_0 + s_1, \end{cases} \quad (23)$$

where b_{n1} and \tilde{N}_{lmn}^2 are given by

$$b_{n1} = \frac{a_{n1}}{a_{n0}} = \frac{\cos(K_{n0} s_0 + \gamma_{n0})}{\cos(K_{n1} s_0 + \gamma_{n1})} = - \frac{\sin[K_{n0}(s_0 + 2AD_0)]}{\sin[K_{n1}(s_1 + 2AD_1)]}, \quad (24)$$

$$\tilde{N}_{lmn}^2 = N_{lmn}^2 / |a_{n0}|^2. \quad (25)$$

Equation (23) represents the Green's function for the parallelepiped in Fig. 1 where the source term is placed in the first layer. In case, z_0 belongs to the second layer the expression for the Green's function changes and a new expression for $\eta_{lmn}(t=0)$ is obtained according to Eqs. (20) and (21). The expression of $\Phi(\mathbf{r}, t)$ for $z_0 > s_0$ is reported in Appendix C. We point out that the position where the isotropic source term is placed does not affect the eigenvalues λ_{lmn} ; therefore, the coefficients K_{n0}^2 or K_{n1}^2 can be obtained as solutions of the transcendental equation (16) in the same way of the case $z_0 < s_0$.

The initial-boundary value problem is thus solved after we determine the discrete number of solutions of the transcendental equation (16). As stated before, here we are looking at the possibility that either K_{n0}^2 or K_{n1}^2 , or both, are negative; therefore, K_{n0} and K_{n1} are imaginary numbers. We notice that imaginary roots of the transcendental equation (16) naturally arise whenever this particular initial-boundary value problem is posed in two or three dimensions. Also in the one-dimensional case (Ref. [32], pp. 335–338), imaginary roots of the transcendental equation are possible if the absorption coefficient is included in the parabolic equation. We note that this case is not treated in Ref. [32]. On the contrary, in two or three dimensions, imaginary roots of the transcendental equation (16) are possible even for nonab-

sorbing layers. The presence of these imaginary roots to the best of our knowledge was not stressed in the literature, despite their fundamental role in the construction of the correct solution (23). In fact, it is possible to demonstrate that the transcendental equation (16) admits always imaginary roots whenever $D_0 \neq D_1$. For the case $D_0 = D_1$, imaginary roots are found only if a minimum criterion for the change in the absorption properties of the two layers $\Delta\mu_a > (\Delta\mu_a)_{min}$ is met.

Let us start to write the relationship between K_{n1}^2 and K_{n0}^2 as

$$K_{n1}^2 = \frac{D_0}{D_1} K_{n0}^2 + C, \quad (26)$$

where

$$C = (\mu_{a0} - \mu_{a1}) / D_1 + K_{lm}^2 (D_0 - D_1) / D_1, \quad (27)$$

$$K_{lm}^2 = K_l^2 + K_m^2.$$

In Fig. 2 the linear relationship between K_{n1}^2 and K_{n0}^2 is shown for $C > 0$ and $C < 0$, respectively. For the case $K_{n0}^2 < -(D_1/D_0)C$ ($C > 0$), or $K_{n0}^2 < 0$ ($C < 0$), possible roots K_{n0} and K_{n1} of Eq. (16) must be imaginary numbers: $K_{n0} = \pm i|K_{n0}|$ and $K_{n1} = \pm i|K_{n1}|$. By using the property $\tanh(z) = -i \tan(iz)$, where z is a complex number, Eq. (16) becomes

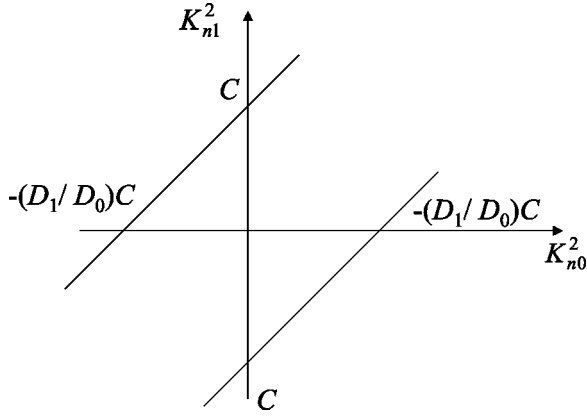


FIG. 2. The linear relationship between K_{n1}^2 and K_{n0}^2 is shown for $C > 0$ (upper line) and $C < 0$ (lower line). The intersections with the axis are also written.

$$\begin{aligned} & \frac{1}{D_0(\pm i|K_{n0}|)} \tanh[\pm|K_{n0}|(s_0 + 2AD_0)] \\ &= -\frac{1}{D_1(\pm i|K_{n1}|)} \tanh[\pm|K_{n1}|(s_1 + 2AD_1)]. \end{aligned} \quad (28)$$

We notice that Eq. (28) is impossible; therefore, our problem cannot admit eigenvalues with both K_{n0}^2 and K_{n1}^2 negative. In terms of the eigenfunctions it means that no eigenfunction has a component along the z axis given by a combination of exponential functions at both sides of the discontinuity $z = s_0$. Let us now treat separately the following two possibilities $C > 0$ and $C < 0$ to search for imaginary roots of Eq. (16).

a. $C > 0$. Possible imaginary roots are found in the interval $-(D_1/D_0)C < K_{n0}^2 < 0$. Here, we are looking at the possibility that Eq. (16) is solved for $K_{n0} = \pm i|K_{n0}|$ and $K_{n1} = \pm|K_{n1}|$. The four different choices for the sign of K_{n0} and K_{n1} yield the same equation

$$\begin{aligned} & -\frac{1}{D_0|K_{n0}|} \tanh[|K_{n0}|(s_0 + 2AD_0)] \\ &= \frac{1}{D_1|K_{n1}|} \tanh[|K_{n1}|(s_1 + 2AD_1)]. \end{aligned} \quad (29)$$

Because we are studying Eq. (29) in a limited interval of K_{n0} and K_{n1} , we notice that a necessary condition for Eq. (29) to admit some roots is

$$\frac{\pi}{2} < \sqrt{C}l_1, \quad (30)$$

where we have defined $l_1 = s_1 + 2AD_1$. A sufficient condition for Eq. (29) to admit some roots is

$$\pi < \sqrt{C}l_1. \quad (31)$$

If $D_0 > D_1$, surely condition (31) will be met for infinite choices of K_l and K_m , and for each one of them Eq. (29) admits a finite number of roots. If we define $\alpha_1 = |K_{n1}|l_1$ and

$M_0 = \text{int}[\sqrt{C}l_1/\pi]$ (“int” indicates the integer part of the division), all the possible roots are found where $\alpha_1 \in \cup_{j=1}^{M_0} ((2j-1)\pi/2, j\pi) \cup (M_0\pi, \sqrt{C}l_1)$ for the case $M_0 > 0$. While for the case $M_0 = 0$, the possible root is found where $\alpha_1 \in (\pi/2, \sqrt{C}l_1)$. It is also possible that there exists at maximum a finite number of choices of K_l and K_m for which condition (30) is not met and therefore there are no roots of Eq. (29).

If $D_0 = D_1 = D$ (when $C > 0$ it means that $\mu_{a0} > \mu_{a1}$), a necessary condition for Eq. (29) to admit a finite number of roots is

$$\frac{\pi}{2} < \sqrt{\left(\frac{\mu_{a0} - \mu_{a1}}{D}\right)} l_1. \quad (32)$$

It means that the change of absorption coefficient between the layers must satisfy the following minimum criterion (necessary condition):

$$\Delta\mu_a = \mu_{a0} - \mu_{a1} > \left(\frac{\pi}{2}\right)^2 \frac{D}{l_1^2}. \quad (33)$$

If $D_0 < D_1$, the condition that we are considering, $C > 0$, is verified only for a finite number of choices of the K_l and K_m . Again Eq. (29) has roots, if condition (31) is satisfied.

b. $C < 0$. Possible imaginary roots are found in the interval $0 < K_{n0}^2 < -(D_1/D_0)C$. In this case, we are searching for roots of Eq. (16) of the kind: $K_{n0} = \pm|K_{n0}|$ and $K_{n1} = \pm i|K_{n1}|$. After substitution in Eq. (16), we obtain

$$\begin{aligned} & \frac{1}{D_0|K_{n0}|} \tanh[|K_{n0}|(s_0 + 2AD_0)] \\ &= -\frac{1}{D_1|K_{n1}|} \tanh[|K_{n1}|(s_1 + 2AD_1)]. \end{aligned} \quad (34)$$

Necessary and sufficient conditions for Eq. (34) to admit some roots are

$$\frac{\pi}{2} < \sqrt{-\left(\frac{D_1}{D_0}\right)} Cl_0, \quad (35)$$

$$\pi < \sqrt{-\left(\frac{D_1}{D_0}\right)} Cl_0, \quad (36)$$

respectively, where we have defined $l_0 = s_0 + 2AD_0$.

If $D_0 < D_1$, surely condition (36) will be met for infinite choices of K_l and K_m , and for each one of them Eq. (34) admits a finite number of roots. If we define $\alpha_0 = |K_{n0}|l_0$ and $M_0 = \text{int}[\sqrt{-(D_1/D_0)Cl_0}/\pi]$, all the possible roots are found where $\alpha_0 \in \cup_{j=1}^{M_0} ((2j-1)\pi/2, j\pi) \cup (M_0\pi, \sqrt{-(D_1/D_0)Cl_0})$ for the case $M_0 > 0$. While for the case $M_0 = 0$, the possible root is found when $\alpha_0 \in (\pi/2, \sqrt{-(D_1/D_0)Cl_0})$. It is also possible that there exists at maximum a finite number of choices of K_l and K_m for which condition (35) is not met and therefore there are no roots of Eq. (34).

If $D_0 = D_1 = D$ (it means that $\mu_{a0} < \mu_{a1}$), condition (35) yields a necessary condition for the change in the absorption properties of the two layers:

$$\Delta\mu_a = (\mu_{a1} - \mu_{a0}) > \frac{D}{l_0^2} \left(\frac{\pi}{2} \right)^2. \quad (37)$$

If $D_0 > D_1$, the condition that we are considering, $C < 0$, is verified only for a finite number of choices of K_l and K_m . Again, Eq. (34) has roots, if condition (36) is satisfied.

We can summarize this study by stating that whenever $D_0 \neq D_1$, the transcendental equation (16) always admits imaginary roots for either K_{n0} or K_{n1} . While if $D_0 = D_1$, imaginary roots of Eq. (16) are possible only if $\Delta\mu_a > (\Delta\mu_a)_{min}$, and we have determined necessary (and sufficient) conditions for both cases $C > 0$ and $C < 0$.

Now let us treat again simultaneously the two possibilities $C > 0$ and $C < 0$. If $K_{n0}^2 > 0$ ($C > 0$) or $K_{n0}^2 > -(D_1/D_0)C$ ($C < 0$), we search for real roots of the transcendental equation (16). For this case, we have to solve Eq. (16), and because we are studying it in an interval not bounded, we will always find infinite roots.

Why are the imaginary roots of Eq. (16) so important? If we scan Fig. 2 from left to right we understand that whenever imaginary roots exist, they might yield the lowest eigenvalues and, in particular, the minimum eigenvalue λ_{min} . This is definitely the case if, for example, $\Delta\mu_a = 0$, $D_0 > D_1$, and

$$\pi < \sqrt{C_{min}} l_1, \quad (38)$$

where C_{min} is the value of C calculated for $K_l = K_m = K_1 = (\pi/L)$. It is obvious that the minimum eigenvalue dominates in the series solution (23) (especially, at late time). Therefore, a large error in the shape of the temporal profile is expected if λ_{min} is not properly calculated.

Let us finally discuss about the normalization factor N_{lmn} . Expression (22) was obtained, provided that we had a complete orthonormal set of eigenfunctions, given by Eq. (11). The eigenfunctions $\rho_{lmn}(\mathbf{r})$ are normalized if

$$\begin{aligned} 1 &= \int_{\Omega_e} \rho_{lmn}(\mathbf{r}) \rho_{lmn}^*(\mathbf{r}) d\mathbf{r} \\ &= \int_{\Omega_{0e}} \rho_{0lmn}(\mathbf{r}) \rho_{0lmn}^*(\mathbf{r}) d\mathbf{r} + \int_{\Omega_{1e}} \rho_{1lmn}(\mathbf{r}) \rho_{1lmn}^*(\mathbf{r}) d\mathbf{r}, \end{aligned} \quad (39)$$

where Ω_{0e} and Ω_{1e} are the extrapolated regions of Ω_0 and Ω_1 , respectively. After some calculations, we obtain

$$\begin{aligned} N_{lmn}^2 &= \frac{L^2}{4} \left\{ \left[\frac{l_0}{2} - \frac{\sin(2K_{n0}l_0)}{4K_{n0}} \right] \sin^2(K_{n1}l_1) \right. \\ &\quad \left. + \sin^2(K_{n0}l_0) \left[\frac{l_1}{2} - \frac{\sin(2K_{n1}l_1)}{4K_{n1}} \right] \right\}. \end{aligned} \quad (40)$$

This expression of the normalization factor is valid for Eq. (16) for the case where $K_{n0} = |K_{n0}|$ and $K_{n1} = |K_{n1}|$. For the case $K_{n0} = i|K_{n0}|$ and $K_{n1} = |K_{n1}|$ [Eq. (29)], we have

$$\begin{aligned} N_{lmn}^2 &= \frac{L^2}{4} \left\{ \left[-\frac{l_0}{2} + \frac{\sinh(2|K_{n0}|l_0)}{4|K_{n0}|} \right] \sin^2(K_{n1}l_1) \right. \\ &\quad \left. + \sinh^2(|K_{n0}|l_0) \left[\frac{l_1}{2} - \frac{\sin(2K_{n1}l_1)}{4K_{n1}} \right] \right\}. \end{aligned} \quad (41)$$

Finally, for the case $K_{n0} = |K_{n0}|$ and $K_{n1} = i|K_{n1}|$ [Eq. (34)], we have

$$\begin{aligned} N_{lmn}^2 &= \frac{L^2}{4} \left\{ \left[\frac{l_0}{2} - \frac{\sin(2K_{n0}l_0)}{4K_{n0}} \right] \sinh^2(|K_{n1}|l_1) \right. \\ &\quad \left. - \sin^2(K_{n0}l_0) \left[\frac{l_1}{2} - \frac{\sinh(2|K_{n1}|l_1)}{4|K_{n1}|} \right] \right\}. \end{aligned} \quad (42)$$

We also provide the normalization factors \tilde{N}_{lmn}^2 for Eq. (23):

$$\begin{aligned} \tilde{N}_{lmn}^2 &= \frac{L^2}{4} \left\{ \frac{l_0}{2} - \frac{\sin(2K_{n0}l_0)}{4K_{n0}} + \frac{\sin^2(K_{n0}l_0)}{\sin^2(K_{n1}l_1)} \right. \\ &\quad \left. \times \left[\frac{l_1}{2} - \frac{\sin(2K_{n1}l_1)}{4K_{n1}} \right] \right\}, \end{aligned} \quad (43)$$

$$\begin{aligned} \tilde{N}_{lmn}^2 &= \frac{L^2}{4} \left\{ -\frac{l_0}{2} + \frac{\sinh(2|K_{n0}|l_0)}{4|K_{n0}|} + \frac{\sinh^2(|K_{n0}|l_0)}{\sin^2(K_{n1}l_1)} \right. \\ &\quad \left. \times \left[\frac{l_1}{2} - \frac{\sin(2K_{n1}l_1)}{4K_{n1}} \right] \right\}, \end{aligned} \quad (44)$$

$$\begin{aligned} \tilde{N}_{lmn}^2 &= \frac{L^2}{4} \left\{ \frac{l_0}{2} - \frac{\sin(2K_{n0}l_0)}{4K_{n0}} - \frac{\sin^2(K_{n0}l_0)}{\sinh^2(|K_{n1}|l_1)} \right. \\ &\quad \left. \times \left[\frac{l_1}{2} - \frac{\sinh(2|K_{n1}|l_1)}{4|K_{n1}|} \right] \right\}, \end{aligned} \quad (45)$$

which are valid for the cases where both K_{n0} and K_{n1} are real, when $K_{n0} = i|K_{n0}|$ and $K_{n1} = |K_{n1}|$, and $K_{n0} = |K_{n0}|$ and $K_{n1} = i|K_{n1}|$, respectively.

Finally, we notice that from the expression of the irradiance (23) we can calculate the reflectance $R(\xi, t)$ and the transmittance $T(\zeta, t)$ by using the meaning of the flux vector:

$$R(\xi, t) = \mathbf{J}(\xi, t) \cdot (-\mathbf{k}), \quad (46)$$

$$T(\zeta, t) = \mathbf{J}(\zeta, t) \cdot \mathbf{k},$$

where ξ and ζ are arbitrary points on the surface $z=0$ and $z=s_0+s_1$, respectively, and the flux vector is given by Fick's law; \mathbf{k} is the unit vector along z axis. From Eq. (23), we can derive the following expressions for reflectance (47) and transmittance (48), respectively:

$$R(\xi, t) = - \sum_{l,m,n=1}^{\infty} v D_0 K_{n0} \cos(K_l x) \cos(K_m y) \sin(\gamma_{n0}) \\ \times \cos^*(K_{n0} z_0 + \gamma_{n0}) \exp[-(K_0^2 D_0 + \mu_{a0}) v t] / \tilde{N}_{lmn}^2 \quad (47)$$

$$T(\zeta, t) = \sum_{l,m,n=1}^{\infty} v D_1 K_{n1} \cos(K_l x) \cos(K_m y) b_{n1} \\ \times \sin[K_{n1}(s_0 + s_1) + \gamma_{n1}] \cos^*(K_{n0} z_0 + \gamma_{n0}) \\ \times \exp[-(K_1^2 D_1 + \mu_{a1}) v t] / \tilde{N}_{lmn}^2. \quad (48)$$

The whole procedure described provides the time domain Green's function for a two-layered parallelepiped illuminated by an isotropic light source placed in z_0 . The theory for a three-layered medium is described in Appendix D. When a collimated laser beam (z axis in Fig. 1) is impinging the medium, some approximations need to be introduced. The real source term is substituted either by a line of isotropic sources or by a single isotropic point source located at $\mathbf{r}_0 = (0, 0, z_0)$ as considered in our derivation. The coordinate z_0 is obtained by imposing that the line of isotropic point sources and the single point source have the same first moment [36,37]. In accordance with this assumption if the thickness of the first layer is sufficiently large, we have $z_0 = 1/(\mu_{a0} + \mu'_{s0})$, where μ'_{s0} is the reduced scattering coefficient of the first layer [31] and it results $\mu'_{s0} = 1/(3D_0)$ [38]. Although the more general line source can also be treated, in this paper we restrict our investigation to the single point source. In the following section, comparisons with the results of MC simulations obtained for a pencil light beam show that the assumption introduced to model the light source in the analytical theory [$z_0 = 1/(\mu_{a0} + \mu'_{s0})$] is sufficient to have an excellent agreement between simulations and analytical solutions.

III. RESULTS

The results shown in this section were obtained by a comparison of the exact analytical solution of DE, for a turbid two-layered parallelepiped medium [Eqs. (47) and (48)], with the results of MC simulations. Details about the MC can be found in Refs. [30,39,40]. For MC simulations, mainly we used a scattering function derived from the Mie theory for a spherical particle having size parameter a ($a = 2\pi R/\lambda$, where R is the radius of the sphere and λ the wavelength of light) equal to 10^{-4} and a refractive index mismatch of 1.2. The asymmetry factor g resulted to be 5×10^{-8} . However, we stress that whenever we fixed the values of μ'_s in the different layers, no significant differences were observed between MC results obtained for different combinations of scattering functions and scattering coefficients. We point out that by using our MC code, we could select different scattering functions in the different layers. The program for the solution of the DE is organized according to the details given in the preceding section. It is worth to remind that once a set of eigenvalues is calculated by solving the transcendental

equation (16), we have all the useful information for the calculation of the Green's functions of the system at different source-detector distances. The roots of Eq. (16) have been found with a combination of bisection and Newton-Raphson methods [41]. All the figures reported in this section refer to a refractive index $n_0 = n_1 = 1.4$ of the medium and to a refractive index of the external $n_e = 1$.

In Fig. 3, some comparisons between MC (symbols) and DE (continuous lines) temporal profiles (Green's functions) for the reflectance are shown. They refer to a parallelepiped with $s_1 = 100$ mm, $L = 140$ mm, $\mu_{a0} = \mu_{a1} = 0$, $\mu'_{s0} = 1$ mm $^{-1}$, $\mu'_{s1} = 0.5$ mm $^{-1}$ (crosses) and $\mu'_{s1} = 2$ mm $^{-1}$ (diamonds). Figures 3(a)–(c) refer to a thickness of the first layer s_0 of 2, 4, 8 mm, respectively. The source-detector distance is fixed at $d = 22$ mm. Although the comparisons are shown for nonabsorbing layers the temporal profiles of MC simulation and DE can be scaled for an arbitrary value of the absorption by using the same formula [8]. We notice that the geometry and the values of the optical properties (in the range of interest for biomedical applications) chosen in Fig. 7 yield the same temporal profiles that would be obtained for a laterally infinite medium consisting of a layer of thickness s_0 on top of a semi-infinite medium.

In Fig. 4, the comparison for the reflectance is shown for the case in which the second layer cannot be considered as semi-infinite. While the optical properties of the two layers are the same as those in the previous figure, the source-detector distance is $d = 18$ mm, the thicknesses of the top and bottom layers are $s_0 = 4$ mm and $s_1 = 8$ mm, respectively, and $L = 120$ mm. From the comparison of Figs. 3 and 4, the effect of the lower boundary on light propagation is rather evident. For the curve with $\mu'_{s1} = 0.5$ mm $^{-1}$, we observe a slight discrepancy between the analytical and the MC results. This effect is due to a general limitation of the DE and cannot be ascribed to the theory developed. In fact, the solutions of the DE in a homogeneous slab obtained with the EBC show similar discrepancies on the time-resolved reflectance where the source-receiver distance is large compared with the thickness of the slab.

In Fig. 5, a similar comparison between MC and DE temporal profiles is shown for the transmittance. The optical properties are the same as before, while the thicknesses of the two layers are $s_0 = 16$ mm and $s_1 = 4$ mm, respectively. The curves are calculated at the point $\zeta = (0, 0, s_0 + s_1)$.

In Fig. 6, comparisons of MC and DE reflectance are shown for the case $d = 22$ mm, $s_0 = 4$ mm, $s_1 = 100$ mm, $L = 140$ mm, $\mu'_{s0} = \mu'_{s1} = 1$ mm $^{-1}$, and $\mu_{a0} = 0.01$ mm $^{-1}$ and $\mu_{a1} = 0$ (crosses) or $\mu_{a1} = 0.01$ mm $^{-1}$ and $\mu_{a0} = 0$ (diamonds). We remind that because the scattering properties of the layers are identical, the approximate theory developed in a previous work [30] becomes exact and the results of the two theories converge. However, the improvements of the exact theory are clear from Fig. 7 where a comparison among an MC temporal profile and the results of the approximate and exact theories is shown for the case of reflectance. Also shown in the same figure is the temporal profile obtained by using only the real roots of the transcendental equation (16). It is clear that the imaginary roots of the tran-

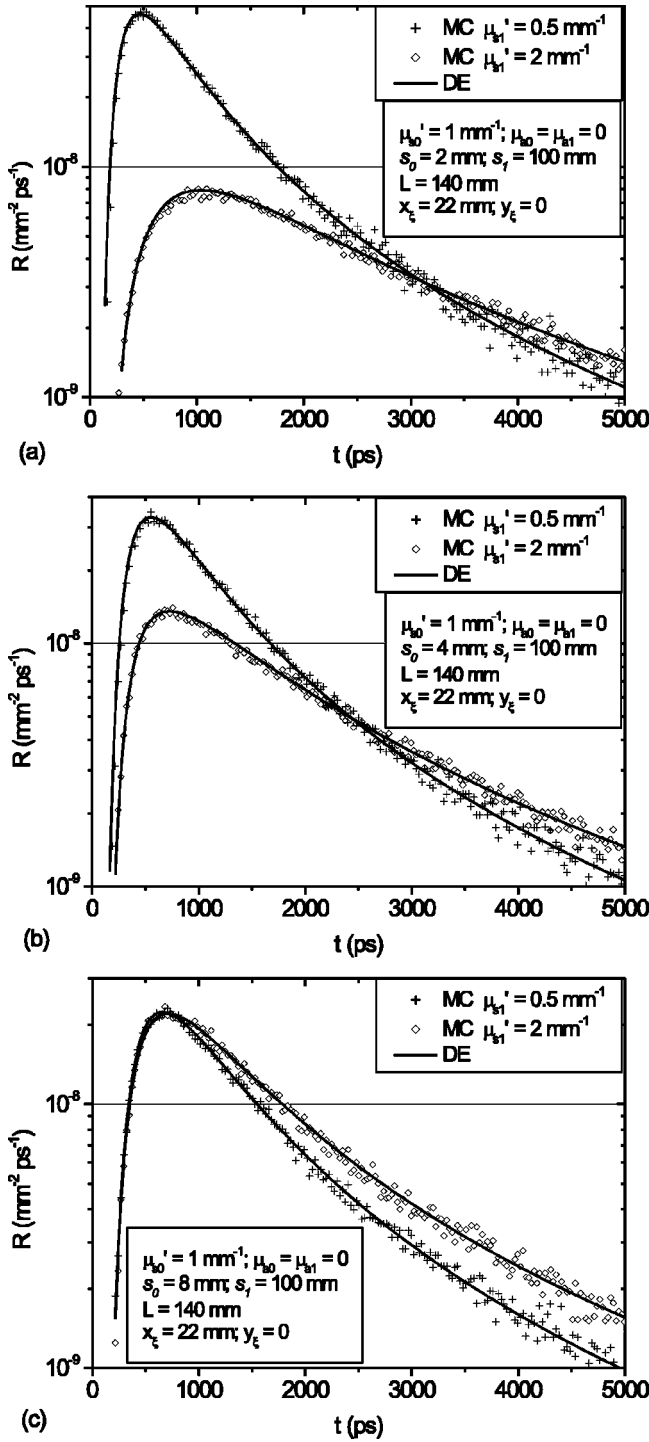


FIG. 3. Reflectance calculated with MC simulations (symbols) and with the solution of DE (continuous lines) for the case of a parallelepiped having $s_1=100$ mm, $L=140$ mm, $\mu_{a0}=\mu_{a1}=0$, $\mu'_{s0}=1$ mm $^{-1}$, $\mu'_{s1}=0.5$ mm $^{-1}$ (crosses), and $\mu'_{s1}=2$ mm $^{-1}$ (diamonds). Parts (a)–(c) refer to the thickness of the first layer s_0 of 2, 4, 8 mm, respectively. The source-detector distance is 22 mm.

scendental equation (16) are fundamental for the correct calculation of formulas (47) and (48). The temporal profiles are calculated at a source-detector distance $d=22$ mm for a medium having $s_0=4$ mm, $s_1=100$ mm, $L=140$ mm, $\mu_{a0}=0.004$ mm $^{-1}$, $\mu_{a1}=0.03$ mm $^{-1}$, $\mu'_{s0}=1$ mm $^{-1}$, and μ'_{s1}

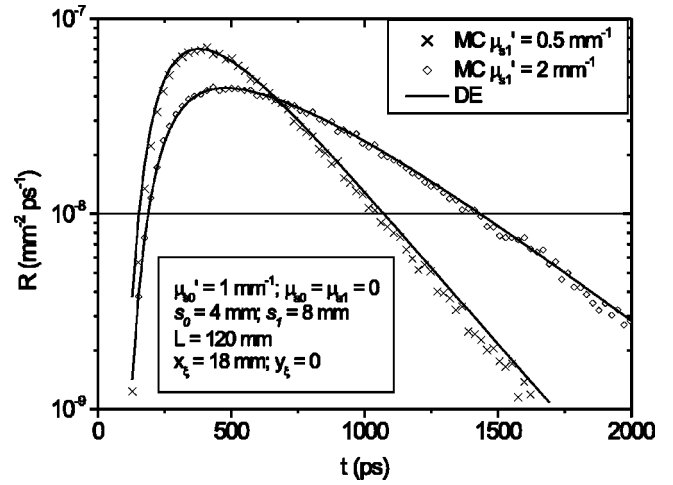


FIG. 4. Reflectance calculated with MC simulations (symbols) and with the solution of DE (continuous lines) for the case of a parallelepiped having $s_0=4$ mm, $s_1=8$ mm, $L=120$ mm, $\mu_{a0}=\mu_{a1}=0$, $\mu'_{s0}=1$ mm $^{-1}$, $\mu'_{s1}=0.5$ mm $^{-1}$ (crosses), and $\mu'_{s1}=2$ mm $^{-1}$ (diamonds). The source-detector distance is 18 mm.

$=0.5$ mm $^{-1}$.

A few remarks are made about the program for the calculation of the DE temporal profiles and about the convergence of the series in Eqs. (47) and (48). If we examine the proposed method and the structure of the transcendental equation (16), we realize that the search of the eigenvalues is mainly affected by the geometry of the medium. In fact, the lateral size of the medium L is related to the “density” of the eigenvalues K_l and K_m , and the thicknesses of the layers, s_0 and s_1 , are connected with the period of the tangent in Eq. (16). All the excellent comparisons presented in this work were obtained by using between 15 and 25 eigenvalues K_l and K_m for the x and y axis, respectively, and for each combination (K_l, K_m) we searched for real roots and possible

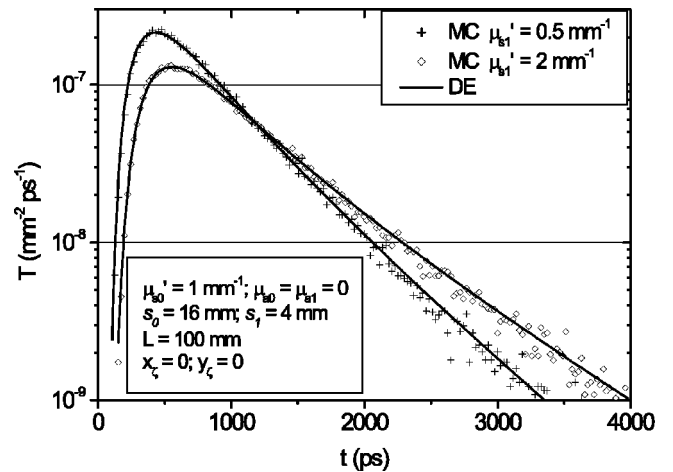


FIG. 5. Transmittance calculated with MC simulations (symbols) and with the solution of DE (continuous lines) for the case of a parallelepiped having $s_0=16$ mm, $s_1=4$ mm, $L=100$ mm, $\mu_{a0}=\mu_{a1}=0$, $\mu'_{s0}=1$ mm $^{-1}$, $\mu'_{s1}=0.5$ mm $^{-1}$ (crosses), and $\mu'_{s1}=2$ mm $^{-1}$ (diamonds). The curves are calculated at the point $\zeta=(0,0,s_0+s_1)$.

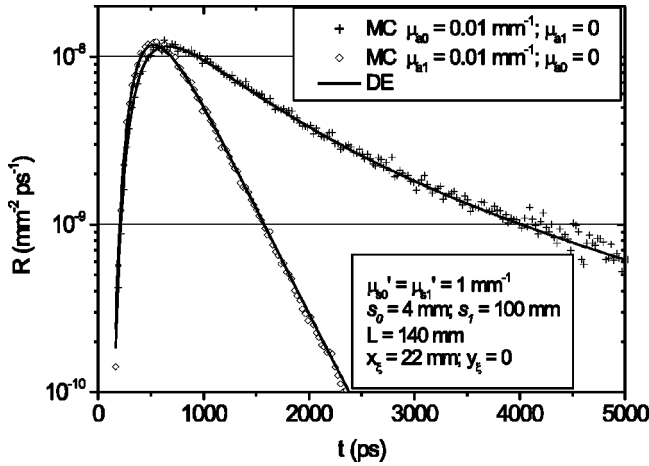


FIG. 6. Reflectance calculated with MC simulations (symbols) and with the solution of DE (continuous lines) for the case of a parallelepiped having $s_0=4$ mm, $s_1=100$ mm, $L=140$ mm, $\mu'_{s0} = \mu'_{s1} = 1$ mm⁻¹, and $\mu_{a0}=0.01$ mm⁻¹ and $\mu_{a1}=0$ (crosses) or $\mu_{a1}=0.01$ mm⁻¹ and $\mu_{a0}=0$ (diamonds). The source-detector distance d is 22 mm.

imaginary roots of the transcendental equation (16) by using standard methods [41]. About the indices l and m the convergence of the series in Eqs. (47) and (48) depends on the lateral dimension of the medium L . For smaller values of L , a lower number of eigenvalues K_l and K_m are required to reach a good convergence. The number of roots K_{n0} and K_{n1} along the z axis necessary to reach the convergence of the series in Eqs. (47) and (48) ranged between 5 and 35 for all the figures. Fewer terms are required when the thicknesses of the two layers are comparable (usually less than 10), whereas more roots are necessary when the thicknesses of the two

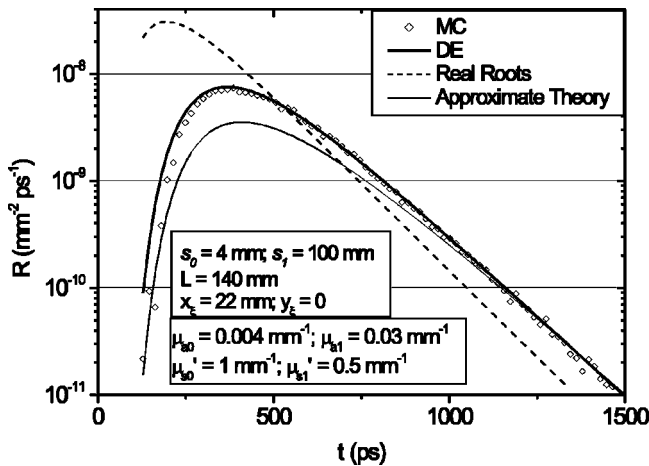


FIG. 7. Reflectance calculated with MC simulations (diamonds) and with the exact solution of DE (thick continuous line) for the case of a parallelepiped having $s_0=4$ mm, $s_1=100$ mm, $L=140$ mm, $\mu_{a0}=0.004$ mm⁻¹, $\mu_{a1}=0.03$ mm⁻¹, $\mu'_{s0} = 1$ mm⁻¹, and $\mu'_{s1} = 0.5$ mm⁻¹. The temporal profiles are calculated at a source-detector distance $d=22$ mm. Also shown are the solution of DE calculated with only the real roots of the transcendental equation (broken line) and the solution of DE calculated with the approximate theory (thin continuous line).

layers are significantly different. The computation time of a set of eigenvalues is proportional to the number of roots required for the convergence of the series in Eqs. (47) and (48). For the cases examined, a set of eigenvalues was calculated in a time always less than 2 s by using a Pentium IV 1.8 GHz.

IV. CONCLUSIONS

An exact expression for the time domain Green’s function solution of the diffusion equation in a layered-parallelepiped has been obtained making use of the eigenfunction method. The proposed method is an extension of the one used in a previous paper [30]. With respect to the previous work, correct boundary conditions between the diffusive layers have been used and a finite geometry has been considered. The key point of the method described in this paper is the solution of a transcendental equation (16) for the eigenvalues that can be accomplished in a short time with classical methods. We stress the importance of imaginary roots of the transcendental equation that, to the best of our knowledge, were not addressed by previous investigators. We have found that without including the imaginary roots of the transcendental equation, the calculation of the Green’s function suffers from the lack of significant terms and consequently the description provided by the formulas can be greatly distorted. The correctness of the analytical expressions for the Green’s functions of a layered parallelepiped has been investigated by comparisons with the results of MC simulations. The results have shown that the analytical solutions are in agreement with the MC results.

The information on the diffusive layered medium can be summarized in a set of eigenvalues that can be calculated in a time of about 1 s. All the quantities of physical interest in any point of the medium are described by this set of eigenvalues. In particular, the Green’s functions at different source-detector distances can be calculated in a very short time. The expression of the Green’s function and its mathematical dependence from the optical properties of the medium is quite straightforward and has an easy interpretation. Moreover, the time integration and the Fourier transform of the Green’s function can be easily carried out to yield analytical expressions for the CW and for the frequency domain.

The formulas were obtained by using the EBC [31] at the upper and lower surfaces of the parallelepiped, but also the more correct partial current boundary condition (PCBC) [42] can be used without any particular problem. The few changes between EBC and PCBC are provided in Appendix E. Rigorous boundary conditions were used between the diffusive layers. The more approximated ZBC [6] was instead used at the lateral surfaces of the parallelepiped, since it simplifies the lateral boundary condition and makes easier to derive the analytical solution for the investigated geometry. The choice of the boundary condition at the lateral boundary does not significantly affect the reflectance or the transmittance, unless the source or the receiver is near to the boundary.

In this paper, we have shown an explicit derivation of the formulas for a two- and a three-layered parallelepiped, but the proposed procedure can be extended to a higher number of layers. It is expected that the complexity of the calcula-

tions required to obtain the Green's function is going to increase with the number of layers considered. We have provided the solution for a layered parallelepiped, but we remark that other finite layered geometries (e.g., cylindrical) can be easily solved with the same method.

Despite the important role played by analytical solutions of the time domain DE, only a few studies presented useful expressions for layered media. On the topic of light propagation through layered random media, there is the lack of rigorous, simple, and explicit analytical expressions that are straightforward to be used for describing photon migration in layered geometries. We also notice that models previously proposed were developed for more restricted geometries. For example, one common element of other models is the requirement that the layered medium is laterally infinitely extended. This paper is intended to provide a flexible and general method for studying light propagation in finite layered media able to overcome some of the drawbacks of other published theories.

In order to see the performance of the analytical solutions for the retrieval of the optical properties of the medium we have performed a preliminary investigation by implementing a fitting procedure based on the formulas presented. We have carried out fitting procedures on measurements simulated with MC results. The convergence of the procedure and the retrieval of the optical properties was obtained in a few minutes. These preliminary results show the potentiality of the formulas to be used in the inverse problem for reconstruction of the optical properties of an unknown medium.

Finally, we would like to point out that the method proposed to solve the DE in the time domain could find several applications for all those physical phenomena that are classifiable as a diffusion process. For instance, we mention the heat transfer through isotropic solid materials for which a similar mathematical approach can be used.

ACKNOWLEDGMENTS

The authors wish to thank Piero Bruscaiglioni for his help and for his useful suggestions. This study was supported in part by the Ministero dell'Università e della Ricerca Scientifica e Tecnologica (MURST) through Progetto Cofinanziato under Grant No. MM02163721.

APPENDIX A: SOLUTION FOR A HOMOGENEOUS CUBE

As an example of the eigenfunction method, let us consider a homogeneous scattering and absorbing cube having side L . We can consider Fig. 1 for the reference system and geometry ($s_0 + s_1 = L$). The time-dependent diffusion equation for a Dirac- δ source term is

$$\left[\frac{1}{v} \frac{\partial}{\partial t} + \mu_a - D \nabla^2 \right] \Phi(\mathbf{r}, t) = \delta(\mathbf{r} - \mathbf{r}_0) \delta(t). \quad (A1)$$

This problem is equivalent to the following initial-boundary value problem:

$$\left[\frac{1}{v} \frac{\partial}{\partial t} + \mu_a - D \nabla^2 \right] \Phi(\mathbf{r}, t) = 0, \quad t > 0 \quad (A2)$$

$$\begin{aligned} \Phi\left(x = \pm \frac{L}{2}, y, z, t\right) &= \Phi\left(x, y = \pm \frac{L}{2}, z, t\right) \\ &= \Phi(x, y, z = 0, t) \\ &= \Phi(x, y, z = L, t) = 0, \end{aligned} \quad (A3)$$

$$\Phi(\mathbf{r}, t = 0) = v \delta(\mathbf{r} - \mathbf{r}_0), \quad (A4)$$

where we have assumed that ZBC is valid throughout the boundary of the cube, and $\mathbf{r}_0 = (0, 0, z_0)$. We will search for a solution of the kind

$$\Phi(\mathbf{r}, t) = \rho(\mathbf{r}) \eta(t). \quad (A5)$$

Substituting Eq. (A5) in Eq. (A2), we get

$$\begin{aligned} d\eta(t)/dt &= -\lambda \eta(t), \\ \nabla^2 \rho(\mathbf{r}) + K^2 \rho(\mathbf{r}) &= 0, \end{aligned} \quad (A6)$$

where $K^2 = (\lambda/v - \mu_a)/D$.

The fact that the diffusion operator $[-D\nabla^2 + \mu_a]$ is positive and self-adjoint implies that $\lambda \geq 0$; however, the Helmholtz equation in system (A6) admits roots also for $K^2 < 0$. The Helmholtz equation can be solved by separation of the variables method. We will search for a solution

$$\rho(\mathbf{r}) = f_l(x) f_m(y) f_n(z). \quad (A7)$$

After substitution of Eq. (A7) in the Helmholtz equation in system (A6), we obtain

$$\begin{aligned} d^2 f_l / (f_l dx^2) &= -K_l^2, \\ d^2 f_m / (f_m dy^2) &= -K_m^2, \\ d^2 f_n / (f_n dz^2) &= -K_n^2, \end{aligned} \quad (A8)$$

where $K^2 = K_l^2 + K_m^2 + K_n^2$. The three equations in system (A8) are formally identical and we can study one of them. Let us consider, for example, the second equation in system (A8). We will treat separately the two cases $K_m^2 > 0$ and $K_m^2 < 0$ as follows.

(a) $K_m^2 > 0$: For this case, the general solution of the equation is

$$f_m(y) = A_m \cos(K_m y + \gamma_m). \quad (A9)$$

Condition (A3) is satisfied, for example, if $K_m = (2m - 1)\pi/L$, $m = 1, 2, 3, \dots$, A_m arbitrary, and $\gamma_m = 0$.

(b) $K_m^2 < 0$: For this case, the general solution is

$$f_m(y) = A_m \exp(p_m y) + B_m \exp(-p_m y), \quad (A10)$$

where A_m and B_m must be determined from the boundary conditions and the parameter p_m verifies $p_m^2 = -K_m^2$. However, condition (A3) can never be satisfied by Eq. (A10), unless $p_m = 0$ and $A_m = -B_m$, and obviously this solution

must be discarded. The same arguments apply for the functions f_l and f_n in Eqs. (A8). We notice that for the function f_n , the constant phase term γ_n is $\gamma_n = \pi/2$. Finally, it is easy to verify that the functions

$$\rho_{lmn}(\mathbf{r}) = \left(\frac{2}{L}\right)^{3/2} [\cos(K_l x) \cos(K_m y) \cos(K_n z + \pi/2)], \quad (\text{A11})$$

with K_l, K_m, K_n given by

$$K_l = (2l-1)\pi/L, \quad l=1,2,3,\dots,$$

$$K_m = (2m-1)\pi/L, \quad m=1,2,3,\dots, \quad (\text{A12})$$

$$K_n = n\pi/L, \quad n=1,2,3,\dots,$$

constitute a complete orthonormal set of eigenfunctions for the cube. In order to find the time-dependent solution in Eqs. (A6), we can apply the same arguments used in Sec. II. Finally, we are led to the following solution of our initial-boundary value problem:

$$\begin{aligned} \Phi(\mathbf{r}, t) = & (2/L)^3 \sum_{l,m,n=1}^{\infty} v \cos(K_l x) \cos(K_m y) \\ & \times \cos(K_n z + \pi/2) \cos(K_n z_0 + \pi/2) \\ & \times \exp[-(K^2 D + \mu_a) v t]. \end{aligned} \quad (\text{A13})$$

APPENDIX B: ORTHONORMALITY OF THE EIGENFUNCTIONS

The orthonormality of two eigenfunctions $\rho_{lmn}(\mathbf{r})$ and $\rho_{l'm'n'}(\mathbf{r})$ (11) can be easily proved for the case $l \neq l'$ or $m \neq m'$; however, when $l=l'$ and $m=m'$ but $n \neq n'$, it requires more calculations. We refer our proof to the solution for a two-layered medium. In the proof for the coefficients l_0 and l_1 , we use the definition in Sec. II. What we have to prove is that

$$\begin{aligned} & \int_{-2AD_0}^{s_0} a_{n0} \cos(K_{n0} z + \gamma_{n0}) a_{n'0}^* \cos^*(K_{n'0} z + \gamma_{n'0}) dz \\ & + \int_{s_0}^{s_0+l_1} a_{n1} \cos(K_{n1} z + \gamma_{n1}) a_{n'1}^* \\ & \times \cos^*(K_{n'1} z + \gamma_{n'1}) dz = I = 0. \end{aligned} \quad (\text{B1})$$

Making use of the Schwarz reflection principle (Ref. [34], p. 391) applied to the cosine function, that is, $\cos^*(z) = \cos(z^*)$, where z is a complex variable, of general properties of the trigonometric functions and of the definition of γ_{n0} and γ_{n1} [see Eq. (14)] the integrals in Eq. (B1) can be calculated as

$$\begin{aligned} I = & (a_{n0} a_{n'0}^*) / [K_{n0}^2 - (K_{n'0}^*)^2] [-K_{n0} \cos(l_0 K_{n0}) \sin(l_0 K_{n'0}^*) \\ & + K_{n'0}^* \sin(l_0 K_{n0}) \cos(l_0 K_{n'0}^*)] \\ & + (a_{n1} a_{n'1}^*) / [K_{n1}^2 - (K_{n'1}^*)^2] \\ & \times [-K_{n1} \cos(l_1 K_{n1}) \sin(l_1 K_{n'1}^*) \\ & + K_{n'1}^* \sin(l_1 K_{n1}) \cos(l_1 K_{n'1}^*)]. \end{aligned} \quad (\text{B2})$$

On the basis of the system of Eqs. (15) and its conjugate system, and on the basis of the relationship between K_{n1}^2 and K_{n0}^2 [see Eq. (26)] and its conjugate we can prove that expression (B2) vanishes. In fact, we have

$$K_{n1}^2 - (K_{n'1}^*)^2 = \frac{D_0}{D_1} [K_{n0}^2 - (K_{n'0}^*)^2], \quad (\text{B3})$$

$$\cos(l_1 K_{n1}) = \frac{a_{n0}}{a_{n1}} \frac{D_0 K_{n0}}{D_1 K_{n1}} \cos(l_0 K_{n0}), \quad (\text{B4})$$

$$\sin(l_1 K_{n'1}^*) = -\frac{a_{n'0}^*}{a_{n'1}^*} \sin(l_0 K_{n'0}^*), \quad (\text{B5})$$

$$\sin(l_1 K_{n1}) = -\frac{a_{n0}}{a_{n1}} \sin(l_0 K_{n0}), \quad (\text{B6})$$

$$\cos(l_1 K_{n'1}^*) = \frac{a_{n'0}^*}{a_{n'1}^*} \frac{D_0 K_{n'0}^*}{D_1 K_{n'1}^*} \cos(l_0 K_{n'0}^*). \quad (\text{B7})$$

To obtain Eq. (B3), we have used the property $(z^*)^2 = (z^2)^*$ and the fact that $C=C'$ [see Eq. (26)]. By substituting expressions (B3)–(B7) in the second term of expression (B2), we obtain the result.

We note that expression (B2) is valid only if $n \neq n'$, and this hypothesis is necessary to prove the orthonormality of the eigenfunctions. However, expression (B2) can also be used for the case $n=n'$ (that is, for the normalization of the eigenfunctions) if we treat K_{n0} and K_{n1} as continuous variables and we calculate the limit for $K_{n0} \rightarrow \pm K_{n'0}^*$ and $K_{n1} \rightarrow \pm K_{n'1}^*$. The double sign depends on the fact that $K_{n'0}^*$ and $K_{n'1}^*$ can be either real or imaginary numbers. In this way we will find the normalization factors given in Sec. II [see Eqs. (40)–(45)]. We point out that the key point of demonstration is the boundary condition between the diffusive layers. In other words, the orthonormality is guaranteed by the boundary conditions assumed. Following a similar approach it is also possible to prove the orthonormality of the solution for a three-layered medium.

APPENDIX C: SOLUTION WITH $z_0 > s_0$

The Green's function for a two-layered parallelepiped when the source term is placed in the second layer, i.e., $z_0 > s_0$, is

$$\Phi(\mathbf{r}, t) = \begin{cases} \sum_{l,m,n=1}^{\infty} v \cos(K_l x) \cos(K_m y) \cos(K_{n0} z + \gamma_{n0}) \\ \times b_{n1}^* \cos^*(K_{n1} z_0 + \gamma_{n1}) \exp[-(K_0^2 D_0 + \mu_{a0}) v t] / \tilde{N}_{lmn}^2, & 0 \leq z \leq s_0 \\ \sum_{l,m,n=1}^{\infty} v \cos(K_l x) \cos(K_m y) b_{n1} \cos(K_{n1} z + \gamma_{n1}) \\ \times b_{n1}^* \cos^*(K_{n1} z_0 + \gamma_{n1}) \exp[-(K_1^2 D_1 + \mu_{a1}) v t] / \tilde{N}_{lmn}^2, & s_0 \leq z \leq s_0 + s_1. \end{cases} \quad (\text{C1})$$

The expression of \tilde{N}_{lmn}^2 changes according to Eqs. (C1) and (39).

APPENDIX D: SOLUTION FOR A THREE-LAYERED PARALLELEPIPED

Let us consider a parallelepiped medium composed by three layers. Referring to Fig. 1 the planes across which the optical properties are discontinuous are $z = s_0$ and $z = s_0 + s_1$. The total thickness of the medium is $s = s_0 + s_1 + s_2$ and the lateral size is L . The optical properties of the three layers are μ_{a0} , D_0 , μ_{a1} , D_1 , and μ_{a2} , D_2 for the top, medium, and bottom layers respectively. For the solution of this problem we can apply the same method as described in Sec. II. We have to solve the DE in three regions and apply the ZBC on the lateral surface and the EBC on the bases of the parallelepiped, respectively; moreover, the continuity of the irradiance and of the photon flux must be applied at the planes $z = s_0$ and $z = s_0 + s_1$. After the separation of variables, we search for solutions (eigenfunctions of the problem) of the three Helmholtz equations of the kind

$$\rho_{lmn}(\mathbf{r}) = \frac{1}{N_{lmn}} \times \begin{cases} \rho_{0lmn} = \cos(K_l x) \cos(K_m y) a_{n0} \cos(K_{n0} z + \gamma_{n0}), & 0 \leq z \leq s_0 \\ \rho_{1lmn} = \cos(K_l x) \cos(K_m y) a_{n1} \cos(K_{n1} z + \gamma_{n1}), & s_0 \leq z \leq s_0 + s_1 \\ \rho_{2lmn} = \cos(K_l x) \cos(K_m y) a_{n2} \cos(K_{n2} z + \gamma_{n2}), & s_0 + s_1 \leq z \leq s_0 + s_1 + s_2. \end{cases} \quad (\text{D1})$$

The ZBC applied at the lateral boundary yields the same set of eigenvalues K_l and K_m found in the previous case (12), while the EBC applied to the top and bottom bases yields

$$\gamma_{n0} = 2K_{n0} A D_0 + \pi/2, \quad (\text{D2})$$

$$\gamma_{n2} = -K_{n2}(s_0 + s_1 + s_2 + 2A D_2) + \pi/2.$$

From the continuity of the irradiance and the photon flux at the planes $z = s_0$ and $z = s_0 + s_1$, we derive the following system of transcendental equations:

$$D_0 K_{n0} \tan(K_{n0} s_0 + \gamma_{n0}) = D_1 K_{n1} \tan(K_{n1} s_0 + \gamma_{n1}), \quad (\text{D3})$$

$$D_1 K_{n1} \tan[K_{n1}(s_0 + s_1) + \gamma_{n1}] \\ = D_2 K_{n2} \tan[K_{n2}(s_0 + s_1) + \gamma_{n2}].$$

Moreover, we derive the condition

$$K_0^2 D_0 + \mu_{a0} = K_1^2 D_1 + \mu_{a1} = K_2^2 D_2 + \mu_{a2}, \quad (\text{D4})$$

where K_0^2, K_1^2, K_2^2 are defined by the formulas

$$K_0^2 = K_l^2 + K_m^2 + K_{n0}^2, \quad (\text{D5})$$

$$K_1^2 = K_l^2 + K_m^2 + K_{n1}^2,$$

$$K_2^2 = K_l^2 + K_m^2 + K_{n2}^2.$$

Therefore, we can solve system (D3) for the variables K_{n0} and γ_{n1} . The normalization of the eigenfunctions is carried out in the same way described previously. Applications of the eigenfunctions method for a three-layered slab have been already presented within the approximate theory [30].

APPENDIX E: SOLUTION WITH THE PCBC

A two-layered medium is considered (see Fig. 1). Instead of using the EBC at the surface $z = 0$ and $z = s_0 + s_1$, the PCBC can be used [42]. To use the PCBC, Eq. (14) should be substituted by

$$\gamma_{n0} = -\arctan[1/(2A D_0 K_{n0})], \quad (\text{E1})$$

$$\gamma_{n1} = -K_{n1}(s_0 + s_1) + \arctan[1/(2A D_1 K_{n1})].$$

The fluence rate in the diffusive layers is derived with the same procedure as described in Sec. II, provided the expressions for the normalization factor, Eqs. (40–45), are updated to the PCBC. The expressions for the reflectance and the transmittance are obtained from the expressions for the fluence rate and from the PCBC [42] according to equations

$$R(\xi, t) = [1/(2A)]\Phi(\xi, t),$$

$$T(\zeta, t) = [1/(2A)]\Phi(\zeta, t).$$
(E2)

The same procedure can also be used for a three-layered medium.

-
- [1] S. Chandrasekhar, *Radiative Transfer* (Oxford University Press, London/Dover, New York, 1960).
- [2] A. Ishimaru, *Wave Propagation and Scattering in Random Media* (IEEE Press, New York/Oxford University Press, Oxford, 1997).
- [3] J.J. Duderstadt, *Transport Theory* (Wiley, New York, 1979).
- [4] G.W. Kattawar, G.N. Plass, and S.J. Hitzfelder, *Appl. Opt.* **15**, 632 (1976).
- [5] G.N. Plass, G.W. Kattawar, and F.E. Catchings, *Appl. Opt.* **12**, 314 (1973).
- [6] M.S. Patterson, B. Chance, and B.C. Wilson, *Appl. Opt.* **28**, 2331 (1989).
- [7] J.B. Fishkin and E. Gratton, *J. Opt. Soc. Am. A* **10**, 127 (1993).
- [8] S.R. Arridge, M. Cope, and D.T. Delpy, *Phys. Med. Biol.* **37**, 1531 (1992).
- [9] T.J. Farrell, M.S. Patterson, and M. Essenpreis, *Appl. Opt.* **37**, 1958 (1998).
- [10] M.A. Franceschini, S. Fantini, L.A. Paunescu, J.S. Maier, and E. Gratton, *Appl. Opt.* **37**, 7447 (1998).
- [11] R.J. Hunter, M.S. Patterson, T.J. Farrel, and J.E. Hayward, *Phys. Med. Biol.* **47**, 193 (2002).
- [12] S. Takatani and M.D. Graham, *IEEE Trans. Biomed. Eng.* **26**, 656 (1979).
- [13] J.M. Schmitt, G.X. Zhou, E.C. Walker, and R.T. Wall, *J. Opt. Soc. Am. A* **7**, 2141 (1990).
- [14] I. Dayan, S. Havlin, and G.H. Weiss, *J. Mod. Opt.* **39**, 1567 (1992).
- [15] A. Kienle, M.S. Patterson, N. Dögnitz, R. Bays, G. Wagnieres, and H. Van den Bergh, *Appl. Opt.* **37**, 779 (1998).
- [16] G. Alexandrakis, T.J. Farrel, and M.S. Patterson, *Appl. Opt.* **37**, 7401 (1998).
- [17] M. Kobayashi, Y. Ito, N. Sakauchi, I. Oda, I. Kōnishi, and Y. Tsunazawa, *Opt. Express* **9**, 802 (2001).
- [18] M. Keijer, W.M. Star, and P.R.M. Storch, *Appl. Opt.* **27**, 1820 (1988).
- [19] R. Nossal, J. Kiefer, G.H. Weiss, R. Bonner, H. Taitelbaum, and S. Havlin, *Appl. Opt.* **27**, 3382 (1988).
- [20] H. Taitelbaum, S. Havlin, and G.H. Weiss, *Appl. Opt.* **28**, 2245 (1989).
- [21] G. Alexandrakis, T.J. Farrel, and M.S. Patterson, *Appl. Opt.* **39**, 2235 (2000).
- [22] T.H. Pham, T. Spott, L.O. Svaasand, and B.J. Tromberg, *Appl. Opt.* **39**, 4733 (2000).
- [23] J. Ripoll, V. Ntziachristos, J.P. Culver, D.N. Pattanayak, A.G. Yodh, and M. Nieto-Vesperinas, *J. Opt. Soc. Am. A* **18**, 821 (2001).
- [24] G. Alexandrakis, D.R. Busch, G.W. Faris, and M.S. Patterson, *Appl. Opt.* **40**, 3810 (2001).
- [25] C.K. Hayakawa, J. Spanier, F. Bevilacqua, A.K. Dunn, J.S. You, B.J. Tromberg, and V. Venugopalan, *Opt. Lett.* **26**, 1335 (2001).
- [26] A.H. Hielscher, H. Liu, B. Chance, F.K. Tittel, and S.L. Jacques, *Appl. Opt.* **35**, 719 (1996).
- [27] A. Kienle, T. Glanzman, G. Wagnieres, and H. Van den Bergh, *Appl. Opt.* **37**, 6852 (1998).
- [28] J. Tualle, J. Prat, E. Tinet, and S. Avrillier, *J. Opt. Soc. Am. A* **17**, 2046 (2000).
- [29] A. Pifferi, A. Torricelli, P. Taroni, and R. Cubeddu, *Opt. Lett.* **26**, 1963 (2001).
- [30] F. Martelli, A. Sassaroli, Y. Yamada, G. Zaccanti, *J. Opt. Soc. Am. A* **19**, 71 (2002).
- [31] D. Contini, F. Martelli, and G. Zaccanti, *Appl. Opt.* **36**, 4587 (1997).
- [32] E. Zauderer, *Partial Differential Equations of Applied Mathematics*, 2nd ed. (Wiley-Interscience, New York, 1989).
- [33] G.F. Roach, *Green Functions: Introductory Theory with Applications* (Van Nostrand Reinhold, London, 1970).
- [34] G.B. Arfken and H.J. Weber, *Mathematical Methods for Physicists*, 4th ed. (Academic Press, New York, 1995).
- [35] R. Aronson, *J. Opt. Soc. Am. A* **12**, 2532 (1995).
- [36] D.R. Wyman, M.S. Patterson, and B.C. Wilson, *J. Comput. Phys.* **81**, 137 (1989).
- [37] E.L. Hull and T.H. Foster, *J. Opt. Soc. Am. A* **18**, 584 (2001).
- [38] K. Furutsu and Y. Yamada, *Phys. Rev. E* **50**, 3634 (1994).
- [39] G. Zaccanti, *Appl. Opt.* **30**, 2031 (1991).
- [40] F. Martelli, D. Contini, A. Taddeucci, and G. Zaccanti, *Appl. Opt.* **36**, 4600 (1996).
- [41] W.H. Press, B.P. Flannery, S.A. Teukolsky, and W.T. Vetterling, *Numerical Recipes: The Art of Scientific Computing* (Cambridge University Press, Cambridge, U.K., 1988).
- [42] R.C. Haskell, L.O. Tsay, T.T. Svaasand, T.C. Feng, M.S. McAdams, and B.J. Tromberg, *J. Opt. Soc. Am. A* **11**, 2727 (1994).